nature chemistry

Article

https://doi.org/10.1038/s41557-023-01225-x

Efficient photon upconversion enabled by strong coupling between silicon quantum dots and anthracene

Received: 29 June 2022

Accepted: 28 April 2023

Published online: 12 June 2023

Check for updates

Kefu Wang[1,2,6], R. Peyton Cline[3,6], Joseph Schwan[4,6], Jacob M. Strain[5], Sean T. Roberts[5] ✉, Lorenzo Mangolini[4] ✉, Joel D. Eaves[3] ✉ & Ming Lee Tang[1,2] ✉

Hybrid structures formed between organic molecules and inorganic quantum dots can accomplish unique photophysical transformations by taking advantage of their disparate properties. The electronic coupling between these materials is typically weak, leading photoexcited charge carriers to spatially localize to the dot or to a molecule at its surface. However, we show that by converting a chemical linker that covalently binds anthracene molecules to silicon quantum dots from a carbon–carbon single bond to a double bond, we access a strong coupling regime where excited carriers spatially delocalize across both anthracene and silicon. By pushing the system to delocalize, we design a photon upconversion system with a higher efficiency (17.2%) and lower threshold intensity (0.5 W cm^{-2}) than that of a corresponding weakly coupled system. Our results show that strong coupling between molecules and nanostructures achieved through targeted linking chemistry provides a complementary route for tailoring properties in materials for light-driven applications.

In recent years, researchers have functionalized quantum dots (QDs) with molecules to generate new hybrid materials[1–5] for applications in solar energy harvesting[6–9], catalysis[10–14] and light emission[15–17]. These structures combine advantageous electronic properties of QDs, which possess high absorption cross-sections and size-tunable optical gaps, with those of molecules, which can exhibit high energy transfer efficiencies and specific chemical reactivities. In hybrid structures, charge and energy transfer between QDs and molecules at their surfaces is critical to their function. Typically, molecules are adhered to QDs via non-covalent van der Waals or ionic interactions. Such weak bonding implies weak electronic coupling between them. In the weak coupling regime, the wavefunctions of excited charge carriers are spatially localized to either the QD or surface-anchored molecules. Because electronic coherences are short-lived in the weak coupling limit, energy or charge moves between QDs and molecules via discrete, incoherent hops, as described in theories developed by Marcus[18], Förster[19] and Dexter[20].

However, if the electronic coupling between a QD and a molecule can be amplified, fundamentally different electronic states can emerge. Due to hybridization of their electronic wavefunctions, charge carriers are simultaneously shared between the molecule and QD. In this strong coupling regime, a QD and surface-anchored molecules do not behave as separate entities, but rather as a single material whose electronic properties are distinct from those of its individual components. In the solid state, this scenario is analogous to the formation of an alloy, where strong electronic coupling between distinct atoms yields a new material with a unique functionality. Although strong coupling has been reported between the valence band states of CdSe QDs and the

[1]Department of Chemistry, University of Utah, Salt Lake City, UT, USA. [2]Department of Chemistry, University of California, Riverside, Riverside, CA, USA. [3]Department of Chemistry, University of Colorado Boulder, Boulder, CO, USA. [4]Department of Mechanical Engineering, University of California, Riverside, Riverside, CA, USA. [5]Department of Chemistry, The University of Texas at Austin, Austin, TX, USA. [6]These authors contributed equally: Kefu Wang, R. Peyton Cline, Joseph Schwan. ✉e-mail: roberts@cm.utexas.edu; lmangolini@engr.ucr.edu; Joel.Eaves@colorado.edu; minglee.tang@utah.edu

valence orbitals of phenyldithiocarbamate and carbene ligands[21,22], these reports have demonstrated an impact only on charge transfer rather than energy transfer[23]. While efforts to increase the electronic coupling between QDs and molecules have yielded improved energy transfer rates[24,25], none have surpassed the weak coupling regime as evidenced by the appearance of spatially localized and distinct QD and molecular states in transient absorption experiments.

In this article, we demonstrate that by controlling the structure of carbon bridges that anchor anthracene molecules to silicon QDs, we produce strongly coupled triplet excitons—spin-1 electron–hole bound states—that spatially delocalize across both materials. Triplet states in QD:molecule hybrid systems hold strong interest due to their utility in photon upconversion systems that convert red-to-near-infrared light into ultraviolet-to-visible emission[2,3,11,16,17,26,27]. In these systems, QD:molecule hybrids function as sensitizers that absorb long-wavelength photons and pass their energy in the form of triplet excitons to emitter molecules in solution. Pairs of these excited emitters subsequently pool their energy to produce short-wavelength emission via triplet fusion.

By using a π-conjugated carbon bridge to link anthracene molecules to silicon QDs, we create a strongly coupled hybrid. This enhanced coupling impacts both the energy and spatial distribution of spin-triplet excitons formed by this system, as evidenced by measurable effects in steady-state and time-resolved optical experiments, as well as in electronic structure calculations that all differ qualitatively from those of systems lacking strong coupling. By varying the energy of strongly coupled triplet excitons via altering the number of anthracene molecules that couple to silicon QDs, we design a photon upconversion system that converts green light to blue, achieving an efficiency (17.2%) and threshold power (0.5 W cm^{-2}) that surpass values obtained for prior silicon-QD-based systems[28]. This system's efficiency also compares favourably with the best values achieved to date for QD-based upconversion systems[1].

Our results represent an example of a QD:molecule system that exhibits strongly coupled excitonic states with well-defined triplet character. For hybrid QD:molecule systems, strong coupling can be advantageous both because it allows for tunability over their electronic properties and because, through coherence, it can bypass metastable intermediates in energy or charge transfer that lead to loss pathways. We anticipate that the silicon-QD:anthracene system we report, which employs extended π-conjugation between silicon and carbon to achieve exciton delocalization, can be used to produce strongly coupled nanoscale objects with designer electronic properties for applications in energy conversion, optoelectronics and catalysis.

Results

Silicon QDs were selected for this work as we hypothesized their ability to form strong, covalent bonds with carbon where electrons are equally shared[29,30] would allow for increased electronic coupling between them and molecules anchored to their surface. This ability sets silicon apart from other common QD materials, such as CdSe and PbS, which coordinate molecules to their surface via ionic interactions wherein electrons are localized on one side of the QD:molecule bridge[3]. Silicon QDs with an average diameter of 3.1 nm were prepared via a non-thermal plasma synthesis and functionalized in-flight with 1-dodecene to yield dodecane-capped silicon QDs (Si:dodecane) that were soluble in hydrophobic solvents[31,32]. Si:dodecane was subsequently hydrosilylated with 9-ethynylanthracene, yielding silicon QDs functionalized with a mixture of aliphatic dodecane and 9-vinylanthracene ligands. We refer to these surface-functionalized QDs as Si:9VA (Fig. 1). As a control, a second set of silicon QDs was prepared by replacing 9-ethynylanthracene with 9-vinylanthracene, which yielded silicon QDs with anthracene ligands attached by a two-carbon chain whose carbon atoms were sp^3 hybridized rather than sp^2. We refer to this control sample as Si:9EA (Fig. 1).

Figure 1 shows absorption spectra of Si:dodecane, Si:9EA and Si:9VA in toluene. The absorption spectrum of Si:dodecane is relatively featureless (Fig. 1, grey dashed line), reflecting the indirect bandgap of silicon. In the spectrum of Si:9EA (Fig. 1, blue), a series of resonances appear at 396, 375 and 356 nm that correspond to the vibrational fine structure of the $S_0 \rightarrow S_1$ transition of 9-ethylanthracene (9EA) molecules bound to silicon. As noted in prior work[28], these resonances are slightly redshifted relative to corresponding features in the absorption spectrum of 9-methylanthracene (9MA; Fig. 1, inset), but otherwise do not differ in their linewidth or oscillator strength, indicating that the electronic coupling between 9EA molecules and the silicon QDs to which they are bound is weak.

In contrast to 9EA, 9-vinylanthracene (9VA) molecules display distinctly different behaviour. Upon binding to silicon, each of the absorption peaks that form the vibrational substructure of 9VA's $S_0 \rightarrow S_1$ transition shows substantial broadening (Fig. 1, red). The extended π-conjugation of Si:9VA's sp^2 linkage is expected to facilitate spatial overlap of states involving 9VA's π-electrons and those of silicon, improving their electronic coupling. If sufficiently strong, this coupling can induce partial hybridization of the valence states of 9VA with several silicon states, leading each isolated 9VA absorption resonance to broaden into a band of states with mixed silicon:anthracene character. Thus, the spectral broadening we observe is suggestive of improved silicon:anthracene coupling in Si:9VA with respect to Si:9EA (Fig. 1, inset).

We hypothesized that the stronger coupling present in Si:9VA would improve its ability to shuttle energy between its silicon QD core and anthracene molecules at its surface, which in turn should lead to its superior performance in triplet-fusion-based photon upconversion systems (Fig. 2a). In these systems, photons absorbed by Si:9VA are used to produce excitons with spin-triplet character. For silicon QDs of the size we employ (3.1 nm diameter), prior computational work has predicted the exchange splitting between their optically bright exciton states and dark spin-triplet states is small, ~10 meV (ref. 33). Once formed, triplet excitons can be passed from Si:9VA to emitter molecules diffusing in solution. Diffusive encounters between pairs of excited emitters can allow them to undergo triplet fusion, producing a high-energy, luminescent spin-singlet state.

Figure 2b plots emission spectra obtained from toluene solutions containing Si:9VA and one of two known emitters, 9,10-diphenylanthacene (DPA) or 2,5,8,11-tetra-*tert*-butylperylene (tBu$_4$P). Previously, we showed Si:9EA can efficiently drive triplet exciton transfer to DPA, fuelling production of upconverted light with 7% efficiency[28]. We note the in-flight functionalized Si QDs we employ for this work have allowed us to improve that yield to 15.8%. By contrast, we find Si:9VA particles achieve a paltry upconversion quantum efficiency of only 0.03% when paired with DPA (Fig. 2b, blue). This result appears to go against our expectation that stronger coupling between anthracene and silicon in Si:9VA should lead to improved energy transfer.

As photon upconversion involves multiple energy transfer steps, to identify which step was responsible for the reduced performance of Si:9VA, we replaced DPA in our upconversion system with tBu$_4$P. Doing so produces an upconversion yield, 2.7%, that is over two orders of magnitude larger than that observed when pairing Si:9VA with DPA. This result suggests it is not energy transfer from silicon to 9VA that limits the DPA upconversion system, but rather energy transfer from Si:9VA to DPA. Importantly, DPA and tBu$_4$P possess different triplet energies of 1.77 eV (ref. 34) and 1.53 eV (refs. 34–38), respectively. While anthracene has a triplet energy of 1.8 eV (refs. 34,39), which is just high enough in energy to sensitize triplet energy transfer to DPA, if this energy is lowered in Si:9VA due to coupling to silicon, the lowered energy will hinder the Si:9VA's ability to transfer energy to DPA while having a smaller impact on energy transfer to tBu$_4$P.

To evaluate if the sp^2 bridge of Si:9VA lowers its triplet exciton energy below that of Si:9EA, we examined the electronic structure

https://doi.org/10.1038/s41557-023-01225-x

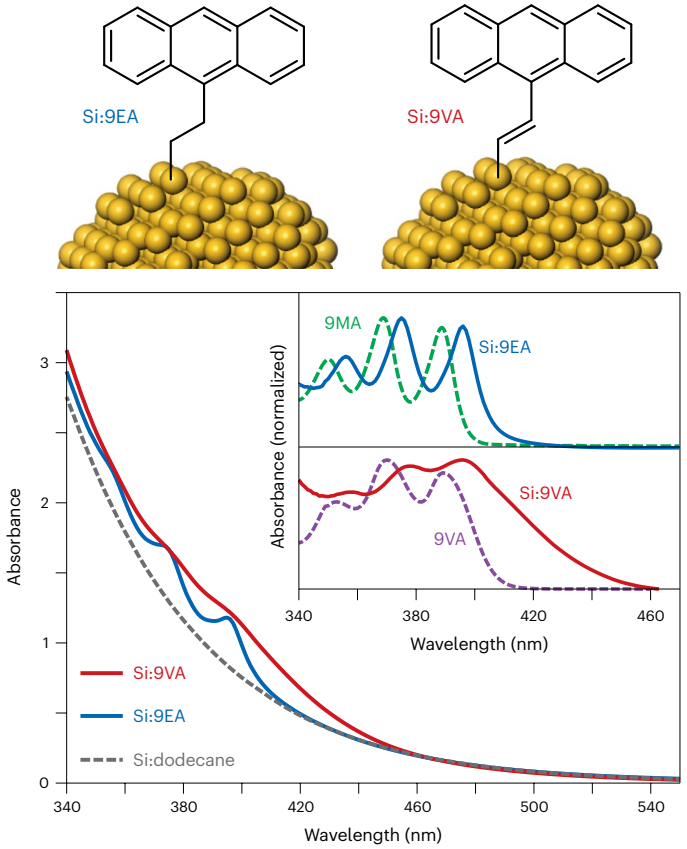

Fig. 1 | Structure and absorption spectra of Si QDs. Structures of Si:9EA and Si:9VA (top). Absorption spectra of Si:dodecane (grey dashed line), Si:9EA (blue, $\langle N_{9EA} \rangle = 3.0$) and Si:9VA (red, $\langle N_{9VA} \rangle = 5.3$) in toluene (bottom). The inset shows the absorption spectra of 9MA and 9VA after subtracting the Si:dodecane background. 9MA and 9VA serve as molecular references for surface-anchored anthracene molecules in Si:9EA and Si:9VA, respectively. The broadening of the resonances in Si:9VA is one indication of strong coupling.

of both materials using density functional theory (DFT). We chose a balance between computational burden and faithful reproduction of experimental systems by creating a two-dimensional periodic slab that was quantum confined in one direction—parallel to the surface normal vector—to mimic the QD diameter. The silicon atoms along the surface normal vector span roughly 2 nm in length, which is comparable to the experimental QD diameter. Each side of the silicon slab is terminated by a Si(111) surface to which a single 9VA or 9EA molecule is attached (Fig. 3). We chose to employ this surface as it corresponds to silicon's lowest-energy surface facet[40–43]. To mimic a silicon QD, we use a slab composed of six crystalline layers, periodically replicated in two dimensions. As we are interested in triplet exciton states, we compute the solutions of the Kohn–Sham equations for the triplets in each Si(111):molecule system using spin-polarized DFT and compute the approximate exciton density of states (DOS) from the conduction and valence bands[44–46].

Figure 3a displays the DOS of triplet excitons computed for both Si(111):9EA and Si(111):9VA. To identify states involving surface-bound anthracene molecules, we projected out contributions to each computed state from the *p* orbitals of the carbon atoms of 9EA and 9VA. In the absence of electronic coupling between silicon and anthracene, the DOS involving these orbitals will be sparse and sharply peaked, just as they are in individual anthracene molecules where large energy gaps separate each of their triplet states. However, if anthracene couples to silicon, the localized states of the molecule will hybridize with several states of the silicon, spreading spatially and energetically, creating a new band of states with mixed silicon:anthracene character. The greater the shifting and broadening of the molecular peaks is, the greater the strength of the coupling between the molecule and silicon will be.

By calculating the projected DOS from the carbon *p* orbitals, we find for Si:9EA (Fig. 3a, blue) that the states fall within a narrow range in energy, indicating that 9EA only weakly couples to silicon. By comparison, the projected DOS broadens substantially for Si:9VA, indicating stronger coupling between anthracene and silicon in this system (Fig. 3a, red). As expected, this coupling shifts the energy of the triplet states involving anthracene in Si:9VA, lowering it below the energy of these states in Si:9EA. This is in accordance with our photon upconversion results, which suggest the triplet exciton energy of Si:9VA is lower than that of Si:9EA (Fig. 2b).

To further explore how silicon:anthracene electronic coupling in Si:9VA and Si:9EA impacts the spatial distribution of their excitonic states, we computed the band-decomposed 'partial' charge densities for triplet states containing carbon *p*-orbital character. In Fig. 3b,c, we plot the contribution of holes to these states for Si:9EA and Si:9VA

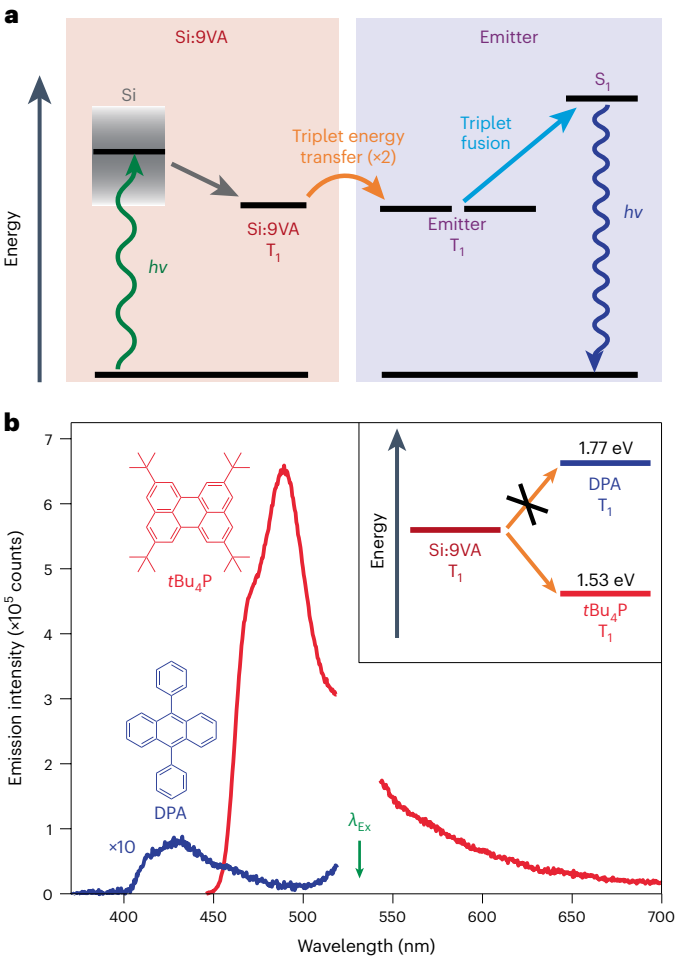

Fig. 2 | State energies and upconversion emission spectra of Si:9VA. a, Energy level diagram illustrating photon upconversion in Si:9VA. Photons absorbed by Si:9VA fuel the transfer of triplet excitons to emitter molecules that subsequently undergo triplet fusion to produce emissive, high-energy, spin-singlet states. *h*, Planck's constant; *ν*, frequency. **b**, Emission spectra (excitation wavelength, $\lambda_{Ex} = 532$ nm) of mixtures of Si:9VA ($\langle N_{9VA} \rangle = 7.3$) with DPA (5.2 mM, blue) and tBu$_4$P (5.2 mM, red; chemical structures are shown as insets). While negligible upconversion is obtained from DPA, efficient upconversion is seen from tBu$_4$P. The upper right inset shows an energy level diagram highlighting that a decrease in Si:9VA's triplet exciton energy due to strong coupling will hinder energy transfer to DPA while still allowing energy transfer to tBu$_4$P.

https://doi.org/10.1038/s41557-023-01225-x

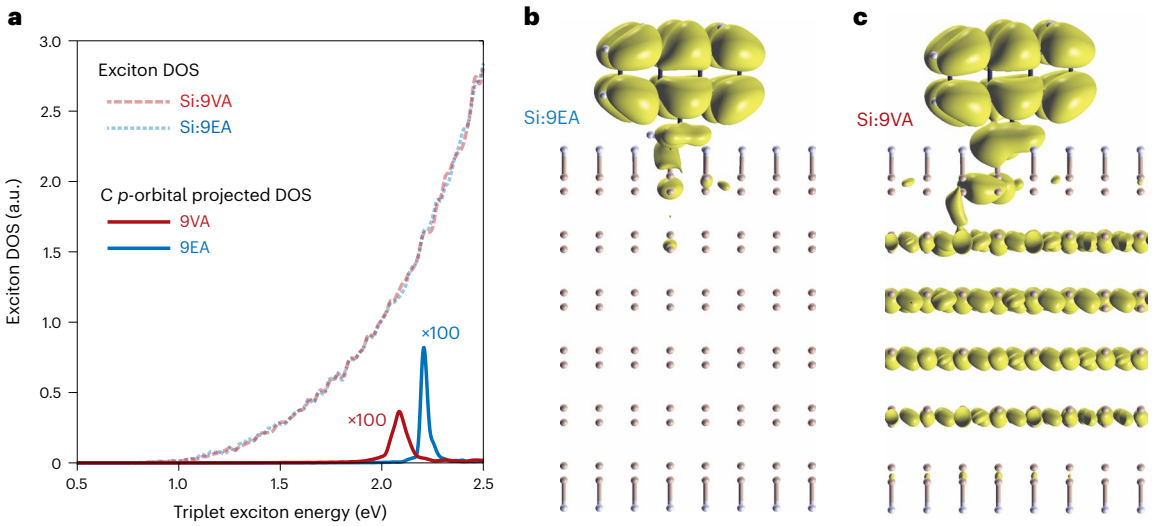

Fig. 3 | Computed electronic structure of Si:9EA and Si:9VA. a, Density of triplet exciton states computed for Si:9VA (light red dashed line) and Si:9EA (light blue dotted line). Contributions from the carbon *p* orbitals come from the atom projected DOS for 9VA (solid red line) and 9EA (solid blue line). These projections have contributions from the principal frontier orbitals of the anthracene and linker (carbon atom *p*-orbital projected DOS). As the sharp resonances of the molecular states mix with those of the solid, the projected DOS shifts and broadens. **b**,**c**, Band-decomposed 'partial' charge densities that highlight the contribution of holes to excitonic states that contain substantial carbon *p*-orbital character for Si:9EA (**b**) and Si:9VA (**c**). They display weak mixing between anthracene and silicon states in Si:9EA and strong coupling in Si:9VA. The weak coupling in Si:9EA leads to states that remain localized to anthracene, while the strong coupling in Si:9VA gives rise to delocalized states that span the organic:inorganic interface.

using the XCrySDen software package[47] (Supplementary Section 4 for computational details). While holes remain well localized to 9EA (Fig. 3b), we see substantial extension of charge density across the Si:9VA interface (Fig. 3c). This indicates the electronic coupling in Si:9VA is sufficiently large to push the system into the strong coupling limit, giving rise to triplet exciton states of mixed silicon:anthracene character that spatially delocalize across these two materials.

Experimental results from transient absorption (TA) spectroscopy in Si:9VA are consistent with the qualitative assignments of strong coupling from DFT. Previously, we showed that photoexcitation of silicon QDs functionalized with 9EA produces a QD-centred triplet exciton state that transfers from silicon to 9EA on a 15.2 ns timescale[28]. This transfer occurs in the weak coupling limit as evidenced by the appearance of an induced absorption band that agrees well with the triplet exciton absorption spectrum of 9MA (Fig. 4a, left and Fig. 4b, blue).

By contrast, we observe fundamentally different behaviour for Si:9VA (Fig. 4a, right). Photoexciting Si:9VA at 532 nm generates charge carriers within the silicon QD, producing a broad induced absorption peak near 950 nm that stems from interband transitions of these carriers. Over a 3 ns timescale, this band decays and a new induced absorption feature centred near 480 nm appears along with a photobleach at wavelengths shorter than 420 nm (Fig. 4b, red). This bleach agrees well with the ground state absorption onset of 9VA molecules that are bonded to silicon (Fig. 1, inset), indicating that the induced absorption band at 480 nm arises from an excited state in which these molecules participate. Notably, this band's spectral lineshape is distinct from that of a triplet excitation localized on 9VA (Supplementary Fig. 5a) and from a charge transfer state wherein an electron or hole has been donated from silicon to 9VA[48,49]. This suggests the generated excited state differs from one wherein charge carriers have been fully transferred from silicon to 9VA. Rather, this band is reminiscent of Fano-type lineshapes that result when the energetically sparse electronic states of a molecule mix with the dense manifold of electronic states of a semiconductor or metal[50,51], signifying strong coupling between 9VA and silicon. This indicates the 3 ns timescale we observe for formation of this state arises not from energy transfer from silicon to 9VA but rather represents the timescale for intersystem crossing that converts a spin-singlet state localized on the silicon QD to a spin-triplet state that spatially extends across the silicon QD:9VA interface (Fig. 4d).

Discussion

Together, our electronic structure calculations and time-resolved measurements indicate that Si:9VA's sp^2 linkage engenders strong coupling between silicon QDs and anthracene and that this coupling acts to lower the triplet exciton energy of this system. With this knowledge in hand, we can fine tune this system's electronic structure to optimize it for photon upconversion. As each 9VA molecule that binds to a silicon QD couples to it strongly, the band of strongly coupled triplet states will widen and shift to lower energy as the number of surface-bound 9VA molecules is increased. Hence, by varying the number of bound 9VA molecules, we expect we can control the energetic position of Si:9VA's lowest-energy triplet exciton state (T_1) and hence set the energetic driving force for triplet exciton transfer from Si:9VA to an upconversion emitter (Fig. 5a).

To test this concept, we measured TA spectra of silicon QDs functionalized with different surface concentrations of 9VA (Fig. 5b). As the average number of surface-bound 9VA molecules, $\langle N_{9VA} \rangle$, is increased from 5.3 to 7.3, we observe a progressive redshift of the photoinduced absorption stemming from Si:9VA's strongly coupled triplet exciton state, from 470 nm to 508 nm. Such a shift is unexpected if the 9VA surface concentration has no impact on Si:9VA's electronic structure. Indeed, for Si:9EA particles wherein anthracene molecules only weakly couple to silicon, we find there is no dependence of the spectral position of the 9EA triplet exciton absorption on the average number of surface-bound 9EA molecules, $\langle N_{9EA} \rangle$ (Supplementary Fig. 6). By contrast, the spectral shift observed in Si:9VA can be explained if increased 9VA surface concentration alters Si:9VA's triplet exciton band structure (Fig. 5b).

Spurred on by our TA results, we optimized the performance of Si:9VA-based photon upconversion systems by varying the energy of Si:9VA's T_1 state by controlling $\langle N_{9VA} \rangle$. Figure 5c,d highlights the performance of upconversion systems that employ DPA and tBu$_4$P emitters, respectively. Whereas Si:9VA particles that bind on average seven 9VA molecules exhibited a miniscule upconversion efficiency of

https://doi.org/10.1038/s41557-023-01225-x

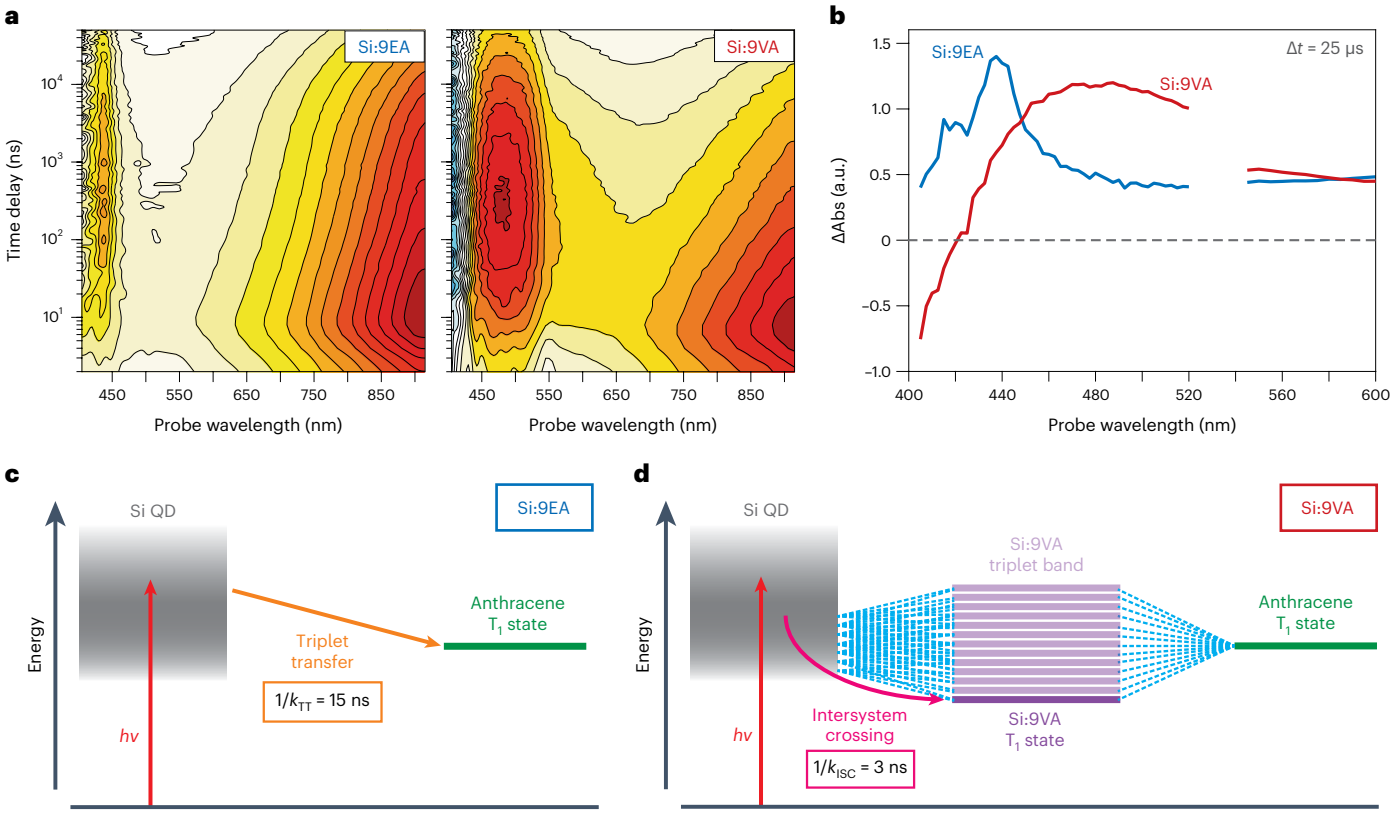

Fig. 4 | Photoexcited kinetics of Si:9EA and Si:9VA. a, TA spectra measured following 532 nm photoexcitation of Si:9EA (left; $\langle N_{9EA} \rangle = 3.0$) and Si:9VA (right; $\langle N_{9VA} \rangle = 5.3$). Red/orange contours represent induced absorption bands while blue contours represent photobleaches, with darker colours denoting stronger signal. **b**, TA spectra recorded at a time delay (Δt) of 25 μs of Si:9EA (blue) and Si:9VA (red). These spectra highlight the nature of the triplet exciton state formed by each system. In Si:9EA, a vibronic progression associated with 9EA's triplet state appears at 438 and 418 nm and signals weak coupling between silicon and 9EA. In Si:9VA, a vibronic progression is not observed. Rather, a broad featureless peak indicates strong electronic coupling between silicon and 9VA. ΔAbs, absorbance change. **c**,**d**, Energy level diagrams illustrating the behaviour of Si:9EA (**c**) and Si:9VA (**d**) following photoexcitation. In Si:9EA, coupling between anthracene and silicon is weak. Photoexcitation of silicon leads to population of a triplet state localized on 9EA on a 15 ns timescale. In Si:9VA, strong coupling between anthracene and silicon gives rise to a band of triplet states with mixed silicon:anthracene character. Photoexcitation of silicon populates the lowest energy state of this band on a 3 ns timescale via intersystem crossing. k_{TT}, triplet exciton transfer rate. k_{ISC}, intersystem crossing rate.

0.03% when paired with DPA (Fig. 2b), we find that reducing $\langle N_{9VA} \rangle$ to 1.8 raises the upconversion efficiency by over two orders of magnitude, to 3.6% (Fig. 5c). We attribute this gain to a reduction in the broadening of Si:9VA's triplet exciton band structure, which raises the energy of Si:9VA's T_1 state and allows it to better donate energy to DPA.

In contrast to behaviour seen for DPA, we find increasing $\langle N_{9VA} \rangle$ from 0.9 to 2.9 enhances photon upconversion by tBu$_4$P (Fig. 5d), which achieves a yield of 17.2% after accounting for inner filter effects (Supplementary Fig. 3). We note that this yield surpasses that of the most efficient silicon-QD-based upconversion system known prior to this work, Si:9EA particles paired with DPA[28]. The performance of Si:9VA paired with tBu$_4$P is even more impressive given that DPA has a higher fluorescence quantum yield than tBu$_4$P (95% versus 70%)[28,52], which means that all things being equal, we would expect DPA-based systems to be roughly a third more efficient at producing upconverted emission than tBu$_4$P-based systems. As Si:9VA and Si:9EA possess similar triplet exciton lifetimes on the order of several tens of microseconds (Supplementary Fig. 8), this performance difference cannot be explained by faster relaxation of excitons within Si:9EA.

Interestingly, increasing $\langle N_{9EA} \rangle$ beyond 2.9 leads to a moderate drop in the upconversion produced by tBu$_4$P. This decrease may stem from a widening of Si:9VA's triplet exciton band structure to a point wherein triplet energy transfer to tBu$_4$P becomes thermally activated or could also result from the formation of low-energy aggregate states between 9VA molecules that directly interact with one another on the particle's surface. Aggregate formation has been reported on the surfaces of SiO_2 particles[53] and implicated in playing a role in both triplet transfer[54] and electron transfer[55,56] between molecules and semiconductors, but assessing the involvement of such states in the photoexcited dynamics of Si:9VA extends beyond the scope of this report.

In summary, by controlling the nature of the chemical bond that affixes anthracene molecules to silicon QDs, we have achieved strong electronic coupling between these materials. Strong coupling enables the formation of triplet exciton states that spatially extend across the silicon:anthracene interface. The energy of these spatially delocalized triplet exciton states can be altered by varying the number of strongly coupled anthracene molecules that bind to silicon. By controlling their energy, we optimize the ability of these states to fuel photon upconversion, achieving an efficiency yield of 17.2% that not only is a record efficiency for silicon-QD-based upconversion systems but ranks among the highest reported for QD-based upconversion systems[1]. More broadly, strong coupling between QDs and molecules provides a complementary handle for tuning the electronic structure of nanomaterials, in addition to changing their size and shape. By delocalizing charge carriers across all molecules bound to a QD, strong coupling can provide unique opportunities for creating systems with an enhanced ability to donate and accept charge, drive chemical transformations and reshape the energy content of light.

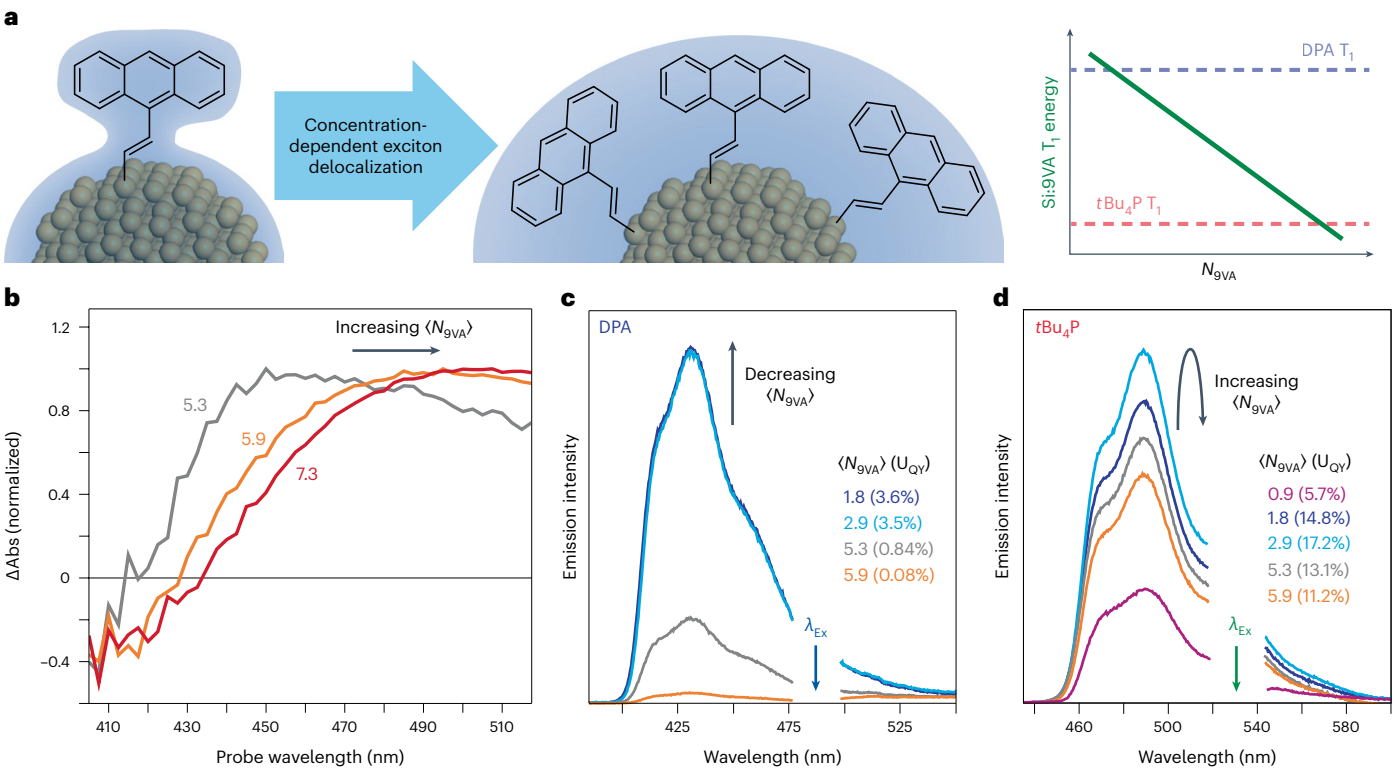

Fig. 5 | Controlling the energy of Si:9VA's T_1 state via strong coupling. **a**, By increasing the number of strongly coupled 9VA molecules that bind to a silicon QD, we can tune the energy of Si:9VA's T_1 state, bringing it into energetic alignment with triplet acceptors. **b**, TA spectra of Si:9VA at a time delay of 25 µs measured as a function of 9VA surface concentration ($\langle N_{9VA}\rangle$ = 5.3, 5.9, 7.3). A redshift of the induced absorption of the Si:9VA triplet exciton band with increasing $\langle N_{9VA}\rangle$ indicates that Si:9VA's T_1 state energy is dependent on the number of 9VA molecules bound to silicon. **c**,**d**, Upconversion emission spectra of DPA (5.2 mM, λ_{Ex} = 485 nm) and tBu$_4$P (5.2 mM, λ_{Ex} = 532 nm) sensitized by Si:9VA particles with differing 9VA surface concentrations. By lowering $\langle N_{9VA}\rangle$ we improve upconversion emission by DPA by raising Si:9VA's T_1 state energy. By raising $\langle N_{9VA}\rangle$, we improve upconversion emission by tBu$_4$P up to a point by lowering Si:9VA's T_1 energy. U_{QY}, upconversion quantum yield.

Online content

Any methods, additional references, Nature Portfolio reporting summaries, source data, extended data, supplementary information, acknowledgements, peer review information; details of author contributions and competing interests; and statements of data and code availability are available at https://doi.org/10.1038/s41557-023-01225-x.

References

1. Brett, M. W., Gordon, C. K., Hardy, J. & Davis, N. J. L. K. The rise and future of discrete organic–inorganic hybrid nanomaterials. *ACS Phys. Chem. Au* **2**, 367–387 (2022).
2. Garakyaraghi, S. & Castellano, F. N. Nanocrystals for triplet sensitization: molecular behavior from quantum-confined materials. *Inorg. Chem.* **57**, 2351–2359 (2018).
3. Huang, Z. & Tang, M. L. Semiconductor nanocrystal light absorbers for photon upconversion. *J. Phys. Chem. Lett.* **9**, 6198–6206 (2018).
4. Frederick, M. T., Amin, V. A. & Weiss, E. A. Optical properties of strongly coupled quantum dot–ligand systems. *J. Phys. Chem. Lett.* **4**, 634–640 (2013).
5. Lu, H. et al. Transforming energy using quantum dots. *Energy Environ. Sci.* **13**, 1347–1376 (2020).
6. Rao, A. & Friend, R. H. Harnessing singlet exciton fission to break the Shockley–Queisser limit. *Nat. Rev. Mater.* **2**, 17063 (2017).
7. Kroupa, D. M. et al. Control of energy flow dynamics between tetracene ligands and PbS quantum dots by size tuning and ligand coverage. *Nano Lett.* **18**, 865–873 (2018).
8. Allardice, J. R. et al. Engineering molecular ligand shells on quantum dots for quantitative harvesting of triplet excitons generated by singlet fission. *J. Am. Chem. Soc.* **141**, 12907–12915 (2019).
9. Lu, H., Chen, X., Anthony, J. E., Johnson, J. C. & Beard, M. C. Sensitizing singlet fission with perovskite nanocrystals. *J. Am. Chem. Soc.* **141**, 4919–4927 (2019).
10. Han, Z., Qiu, F., Eisenberg, R., Holland, P. L. & Krauss, T. D. Robust photogeneration of H_2 in water using semiconductor nanocrystals and a nickel catalyst. *Science* **338**, 1321–1324 (2012).
11. Imperiale, C. J., Green, P. B., Hasham, M. & Wilson, M. W. B. Ultra-small PbS nanocrystals as sensitizers for red-to-blue triplet-fusion upconversion. *Chem. Sci.* **12**, 14111–14120 (2021).
12. Jiang, Y., Wang, C., Rogers, C. R., Kodaimati, M. S. & Weiss, E. A. Regio- and diastereoselective intermolecular [2+2] cycloadditions photocatalysed by quantum dots. *Nat. Chem.* **11**, 1034–1040 (2019).
13. Jiang, Y. & Weiss, E. A. Colloidal quantum dots as photocatalysts for triplet excited state reactions of organic molecules. *J. Am. Chem. Soc.* **142**, 15219–15229 (2020).
14. Brown, K. A., Dayal, S., Ai, X., Rumbles, G. & King, P. W. Controlled assembly of hydrogenase-CdTe nanocrystal hybrids for solar hydrogen production. *J. Am. Chem. Soc.* **132**, 9672–9680 (2010).
15. Mongin, C., Moroz, P., Zamkov, M. & Castellano, F. N. Thermally activated delayed photoluminescence from pyrenyl-functionalized CdSe quantum dots. *Nat. Chem.* **10**, 225–230 (2018).
16. Wu, M. et al. Solid-state infrared-to-visible upconversion sensitized by colloidal nanocrystals. *Nat. Photon.* **10**, 31–34 (2015).

17. Huang, Z. et al. Hybrid molecule–nanocrystal photon upconversion across the visible and near-infrared. *Nano Lett.* **15**, 5552–5557 (2015).
18. Marcus, R. A. On the theory of oxidation-reduction reactions involving electron transfer. I. *J. Chem. Phys.* **24**, 966–978 (1956).
19. Forster, T. Zwischenmolekulare energiewanderung und fluoreszenz. *Ann. Phys.* **6**, 55–75 (1938).
20. Dexter, D. L. A theory of sensitized luminescence in solids. *J. Chem. Phys.* **21**, 836 (1953).
21. Frederick, M. T., Amin, V. A., Cass, L. C. & Weiss, E. A. A molecule to detect and perturb the confinement of charge carriers in quantum dots. *Nano Lett.* **11**, 5455–5460 (2011).
22. Westmoreland, D. E., López-Arteaga, R. & Weiss, E. A. N-heterocyclic carbenes as reversible exciton-delocalizing ligands for photoluminescent quantum dots. *J. Am. Chem. Soc.* **142**, 2690–2696 (2020).
23. Lian, S., Weinberg, D. J., Harris, R. D., Kodaimati, M. S. & Weiss, E. A. Subpicosecond photoinduced hole transfer from a CdS quantum dot to a molecular acceptor bound through an exciton-delocalizing ligand. *ACS Nano* **10**, 6372–6382 (2016).
24. He, S. et al. Engineering sensitized photon upconversion efficiency via nanocrystal wavefunction and molecular geometry. *Angew. Chem. Int. Ed.* **59**, 17726–17731 (2020).
25. Xia, P. et al. On the efficacy of anthracene isomers for triplet transmission from CdSe nanocrystals. *Chem. Commun.* **53**, 1241–1244 (2017).
26. Yanai, N. & Kimizuka, N. New triplet sensitization routes for photon upconversion: thermally activated delayed fluorescence molecules, inorganic nanocrystals, and singlet-to-triplet absorption. *Acc. Chem. Res.* **50**, 2487–2495 (2017).
27. Nienhaus, L. et al. Speed limit for triplet-exciton transfer in solid-state PbS nanocrystal-sensitized photon upconversion. *ACS Nano* **11**, 7848–7857 (2017).
28. Xia, P. et al. Achieving spin-triplet exciton transfer between silicon and molecular acceptors for photon upconversion. *Nat. Chem.* **12**, 137–144 (2020).
29. Carroll, G. M., Limpens, R. & Neale, N. R. Tuning confinement in colloidal silicon nanocrystals with saturated surface ligands. *Nano Lett.* **18**, 3118–3124 (2018).
30. Dohnalova, K., Saeed, S., Poddubny, A. N., Prokofiev, A. A. & Gregorkiewicz, T. Thermally activated emission from direct bandgap-like silicon quantum dots. *ECS J. Solid State Sci. Technol.* **2**, R97–R99 (2013).
31. Anthony, R. J., Cheng, K.-Y., Holman, Z. C., Holmes, R. J. & Kortshagen, U. R. An all-gas-phase approach for the fabrication of silicon nanocrystal light-emitting devices. *Nano Lett.* **12**, 2822–2825 (2012).
32. Li, Z. & Kortshagen, U. R. Aerosol-phase synthesis and processing of luminescent silicon nanocrystals. *Chem. Mater.* **31**, 8451–8458 (2019).
33. Leung, K. & Whaley, K. B. Electron-hole interactions in silicon nanocrystals. *Phys. Rev. B* **56**, 7455–7468 (1997).
34. Montalti, M., Credi, A., Prodi, L. & Gandolfi, M. T. *Handbook of Photochemistry* 3rd edn (CRC Press/Taylor and Francis, 2006).
35. Birks, B. & Slifkin, M. A. π-Electronic excitation and ionization energies of condensed ring aromatic hydrocarbons. *Nature* **191**, 761–764 (1961).
36. Clarke, R. H. & Hochstrasser, R. M. Location and assignment of the lowest triplet state of perylene. *J. Mol. Spectrosc.* **32**, 309–319 (1969).
37. Albrecht, W. G., Michel-Beyerle, M. E. & Yakhot, V. Exciton fission in excimer forming crystal. Dynamics of an excimer build-up in α-perylene. *Chem. Phys.* **35**, 193–200 (1978).
38. Giri, G., Prodhan, S., Pati, Y. A. & Ramasesha, S. A model exact study of the properties of low-lying electronic states of perylene and substituted perylenes. *J. Phys. Chem. A* **122**, 8650–8658 (2018).
39. Evans, D. F. Perturbation of singlet–triplet transitions of aromatic molecules by oxygen under pressure. *J. Chem. Soc.* **1957**, 1351–1357 (1957).
40. Follstaedt, D. M. Relative free energies of Si surfaces. *Appl. Phys. Lett.* **62**, 1116–1118 (1993).
41. Jaccodine, R. J. Surface energy of germanium and silicon. *J. Electrochem. Soc.* **110**, 524 (1963).
42. Eaglesham, D. J., White, A. E., Feldman, L. C., Moriya, N. & Jacobson, D. C. Equilibrium shape of Si. *Phys. Rev. Lett.* **70**, 1643–1646 (1993).
43. Lu, G.-H., Huang, M., Cuma, M. & Liu, F. Relative stability of Si surfaces: a first-principles study. *Surf. Sci.* **588**, 61–70 (2005).
44. Prendergast, D., Grossman, J. C. & Galli, G. The electronic structure of liquid water within density-functional theory. *J. Chem. Phys.* **123**, 014501 (2005).
45. Guerra, J. A., Tejada, A., Töfflinger, J. A., Grieseler, R. & Korte, L. Band-fluctuations model for the fundamental absorption of crystalline and amorphous semiconductors: a dimensionless joint density of states analysis. *J. Phys. D.* **52**, 105303 (2019).
46. O'Leary, S. K. & Malik, S. M. A simplified joint density of states analysis of hydrogenated amorphous silicon. *J. Appl. Phys.* **92**, 4276–4282 (2002).
47. Kokalj, A. Computer graphics and graphical user interfaces as tools in simulations of matter at the atomic scale. *Comput. Mater. Sci.* **28**, 155–168 (2003).
48. Shida, T. & Iwata, S. Electronic spectra of ion radicals and their molecular orbital interpretation. III. Aromatic hydrocarbons. *J. Am. Chem. Soc.* **95**, 3473–3483 (1973).
49. Hiratsuka, H. & Tanizaki, Y. Polarized absorption spectra of aromatic radicals in stretched polymer film. 2. Radical ions of anthracene and pyrene. *J. Phys. Chem.* **83**, 2501–2505 (1979).
50. Fano, U. Effects of configuration interaction on intensities and phase shifts. *Phys. Rev.* **124**, 1866–1878 (1961).
51. Anderson, P. W. Localized magnetic states in metals. *Phys. Rev.* **124**, 41–53 (1961).
52. Fallon, K. J. et al. Molecular engineering of chromophores to enable triplet–triplet annihilation upconversion. *J. Am. Chem. Soc.* **142**, 19917–19925 (2020).
53. Gorman, J. et al. Excimer formation in carboxylic acid-functionalized perylene diimides attached to silicon dioxide nanoparticles. *J. Phys. Chem. C* **123**, 3433–3440 (2019).
54. Huang, Z., Simpson, D. E., Mahboub, M., Li, X. & Tang, M. L. Ligand enhanced upconversion of near-infrared photons with nanocrystal light absorbers. *Chem. Sci.* **7**, 4101–4104 (2016).
55. Zheng, Y. et al. Influence of molecular aggregation on electron transfer at the perylene diimide/indium-tin oxide interface. *ACS Appl. Mater. Interfaces* **8**, 34089–34097 (2016).
56. Cadena, D. M. et al. Aggregation of charge acceptors on nanocrystal surfaces alters rates of photoinduced electron transfer. *J. Am. Chem. Soc.* **144**, 22676–22688 (2022).

Data availability

Source data are provided with this paper. Additional source data for figures contained in the Supplementary Information are available from the authors upon request.

Acknowledgements

This work was supported by National Science Foundation grant CMMI-2053567. Work at the University of Texas at Austin was additionally supported by the Welch Foundation (grant F-1885). Aspects of this work undertaken at the University of Colorado Boulder and the University of Texas at Austin were supported by the W. M. Keck Foundation (grant 22605). Work at the University of California, Riverside was also supported by Air Force Office of Scientific Research grant FA9550-20-1-0112. This work used the Summit supercomputer, which is supported by the National Science Foundation (awards ACI-1532235 and ACI-1532236), the University of Colorado Boulder and Colorado State University. The Summit supercomputer is a joint effort of the University of Colorado Boulder and Colorado State University.

Author contributions

K.W. conducted the nanocrystal functionalization, photon upconversion and nanosecond TA experiments. R.P.C. performed the electronic structure calculations; J.S., the non-thermal plasma synthesis; and J.M.S. the subnanosecond TA. K.W., J.S., L.M. and M.L.T. conceived of the project. R.P.C. and J.D.E. designed the electronic structure calculations. S.T.R. composed the manuscript with substantial contributions from all authors.

Competing interests

The authors declare no competing interests.

Additional information

Supplementary information The online version contains supplementary material available at https://doi.org/10.1038/s41557-023-01225-x.

Correspondence and requests for materials should be addressed to Sean T. Roberts, Lorenzo Mangolini, Joel D. Eaves or Ming Lee Tang.

Peer review information *Nature Chemistry* thanks the anonymous reviewers for their contribution to the peer review of this work.